DOI:
10.2967/jnumed.124.267876
10.2967/jnumed.124.267876

Document Version
Peer reviewed version

In Vivo PET Imaging of ^{89}Zr-Labeled Natural Killer Cells and the Modulating Effects of a Therapeutic Antibody

Authors

Truc T Pham*#, Alicia Chenoweth†‡, Natasha Patel*, Arshiya Banu*, Gabriel Osborn†, Philip J Blower*, Sophia N Karagiannis†‡ and Michelle T Ma*#

*Department of Imaging Chemistry and Biology, School of Bioengineering and Imaging Sciences, King's College London, London, UK

†St. John's Institute of Dermatology, School of Basic & Medical Biosciences, King's College London, London SE1 9RT, United Kingdom

‡Breast Cancer Now Research Unit, School of Cancer & Pharmaceutical Sciences, King's College London, Guy's Hospital, London SE1 9RT, United Kingdom

#Corresponding authors:

Truc T Pham: truc.pham@kcl.ac.uk, ORCID: 0000-0001-5850-4592

Michelle T Ma: michelle.ma@kcl.ac.uk, ORCID: 0000-0002-3349-7346

FINANCIAL STATEMENT: This research was supported by Cancer Research UK (C30122/A11527; C30122/A15774; C4278/A27066; C63178/A24959), the EPSRC (EP/S032789/1), Wellcome Trust (WT212885/Z/18/Z; WT201959/Z/16/Z; WT088641/Z/09/Z), Breast Cancer Now (147KL-Q3) and the MRC (MR/L023091/1, MR/N013700/1). PJB has submitted a patent application related to [^{89}Zr]^{89}Zr-Oxine technology. SNK is a founder and shareholder of Epsilogen Ltd. and declares patents on antibody technologies. No other potential conflicts of interest relevant to this article exist.

Word count: 4979

ABSTRACT

Introduction: Natural Killer (NK) cells can kill cancer cells via antibody-dependent cell-mediated cytotoxicity (ADCC): a tumor-associated IgG antibody binds to the Fcγ Receptor CD16 on NK cells via the antibody Fc region and activates NK cell cytotoxic functions. Here, we employed PET imaging to assess NK cell migration to HER2-positive HCC1954 breast tumors, examining the influence of HER2-targeted trastuzumab antibody treatment on NK cell tumor accumulation.

Methods: Human NK cells from healthy donors were expanded *ex vivo* and labeled with [^{89}Zr]^{89}Zr-Oxine. *In vitro* experiments compared the phenotypic markers, viability, proliferation, migration, degranulation, and ADCC behaviors of both labeled (^{89}Zr-) and unlabeled NK cells. Female NSG mice bearing orthotopic human breast HCC1954 tumors were administered ^{89}Zr-NK cells alongside trastuzumab treatment or a sham treatment, then scanned using PET/CT imaging over 7 days. Flow cytometry and γ-counting were used to analyze the presence of ^{89}Zr-NK cells in liver and spleen tissues.

Results: ^{89}Zr cell radiolabeling yields measured 42.2 ± 8.0%. At an average specific activity of 16.7 ± 4.7 kBq/10^6 cells, ^{89}Zr-NK cells retained phenotypic and functional characteristics including CD56 and CD16 expression, viability, migration, degranulation and ADCC capabilities. *In vivo* PET/CT studies indicated predominant accumulation of ^{89}Zr-NK cells in the liver and spleen. *Ex vivo* analyses of liver and spleen tissues indicated that the administered human ^{89}Zr-NK cells retain their radioactivity *in vivo* and that ^{89}Zr does not transfer to cells of murine soft tissues, thus validating this ^{89}Zr PET method for NK cell tracking. Notably, ^{89}Zr-NK cells migrated to HER2-positive tumors, both with and without trastuzumab treatment. Trastuzumab treatment was associated with increased ^{89}Zr-NK cell signal at days 1 and 3 PI.

Conclusions: *In vitro*, ^{89}Zr-NK cells maintained key cellular and cytotoxic functions. *In vivo*, ^{89}Zr-NK cells trafficked to HER2-postive tumors, with trastuzumab treatment correlating with enhanced ^{89}Zr-NK infiltration. This study demonstrates the feasibility of using PET to image ^{89}Zr-NK cell infiltration to solid tumors.

Key words: Natural Killer cell, ADCC, trastuzumab, HER2 receptor, cell tracking

INTRODUCTION

Monoclonal IgG antibodies (mAbs) used in clinical oncology exert therapeutic effects by inhibiting cancer cell receptors that drive tumor proliferation. In breast cancer treatment, trastuzumab targets the human epidermal growth factor receptor 2 (HER2). By binding of the antibody Fab region to HER2, trastuzumab prevents HER2 dimerization, thus inhibiting the downstream proliferative signals that promote tumor growth. In addition, in combination with immune effector cells (most notably Natural Killer (NK) cells), trastuzumab can trigger Antibody-Dependent Cell-mediated Cytotoxicity (ADCC), resulting in immune cell activation and cancer cell lysis.

NK cells express the low-affinity yet potent FcγRIIIA (or CD16) activating receptor. *In vivo*, a specific IgG mAb can engage via its Fab region with its target antigen on a cancer cell; simultaneously, the Fc region of the mAb is recognized by CD16, facilitating the activation of cytotoxic NK cell functions. NK cells can also *independently* induce cytotoxic responses against cancer cells through lytic synapse formation or apoptotic pathways. They also modulate other immune responses involving T cells, macrophages and dendritic cells, through cytokine or chemokine pathways.

ADCC can contribute to the efficacy of HER2-targeted immunotherapies. In patients administered HER2-targeted immunotherapies, *improved responses* are associated with higher tumor infiltration of NK cells (*1*–*3*) and/or lymphocytes (*4*,*5*) in HER2-positive breast cancer biopsies. Furthermore, analyses of surgical specimens from HER2-positive breast cancers have previously revealed an *increase in NK cells in tumor tissue after trastuzumab treatment*, relative to specimens collected either before treatment (*1*), or from case-matched controls who did not receive trastuzumab treatment (*2*). Similarly, in a murine model of HER2-positive breast cancer, an increase in NK cell numbers was observed in tumors after treatment with a trastuzumab-derived antibody-drug conjugate (ADC) (*6*). Highlighting the clinical significance of ADCC effects mediated by NK cells, a phase 1 clinical trial in patients with HER2-positive tumors recently reported that a therapeutic regime of expanded autologous NK cells in combination with trastuzumab is safe, exhibits tumor engagement and shows preliminary evidence of therapeutic efficacy (*7*). Compared to paired tumor biopsies obtained pre-treatment, increases in NK cells, lymphocytes and apoptosis activity were observed in biopsies post-treatment.

The distribution and tumor infiltration of NK cells, and how this may be influenced by therapeutic antibody treatment, is therefore important in understanding the immunological landscape of cancer, at

the cellular, tissue and whole-body levels. Whole-body imaging can provide spatial and longitudinal insights into the distribution of NK cells *in vivo*. In direct "cell tracking" methods, NK cells are labeled *ex vivo* with a contrast agent and then administered for *in vivo* tracking using whole-body imaging. This approach has been previously applied using optical imaging (*8*,*9*), MRI (*10*), Single Photon Emission Computed Tomography (SPECT) or γ-scintigraphy with [^{111}In]In-oxine (*11–13*), and Positron Emission Tomography (PET) using [^{89}Zr]Zr-oxine (*14*). Optical imaging and MRI can provide high-resolution images but lack quantitative attributes. In contrast, PET and γ-scintigraphy/SPECT imaging can provide real-time and quantitative information, and both are highly sensitive.

A recently developed method enables the radiolabeling of cells using [^{89}Zr]Zr-oxine (^{89}Zr half-life = 78.41 h), facilitating longitudinal cell tracking over 1–2 weeks with PET (*15*): it has been applied to track NK cells (*14*), T cells (*16*,*17*) and bone marrow cells (*18*) *in vivo*, amongst others (*19*). Similar methods using [^{111}In]In-oxine are well-established for ^{111}In cell tracking with γ-scintigraphy/SPECT imaging. In both cases, [^{89}Zr]Zr-oxine and [^{111}In]In-oxine diffuse into cells and release the radionuclide intracellularly, resulting in cell labeling. Previous *in vivo* studies have investigated the biodistribution of ^{89}Zr- and ^{111}In-labeled NK cells in healthy and cancer subjects without the augment of therapeutic adjuvants (*11–14*). Here, we use PET/CT tracking to study the biodistribution of ^{89}Zr-labeled human NK cells in mice bearing HER2-positive solid orthotopic HCC1954 human breast tumors and assess whether administration of HER2-targeted trastuzumab enhances NK cell infiltration into tumors.

MATERIALS AND METHODS

1. Human NK cells, ^{89}Zr-radiolabeling and cell assays

Experiments using human blood received approval from KCL-REC (Study Reference HR/DP-20/21-24483). All donors provided written informed consent. NK cells were isolated from human peripheral blood mononuclear cell layer, cultured, and expanded *ex vivo* (*20*). [^{89}Zr]Zr-oxine (~45 kBq/10^6 cells) was added to *ex vivo* expanded NK cells suspended in PBS at 15–20 x 10^6 cells/mL, followed by incubation for 15 min at ambient temperature (*15*) (see Supplemental Data).

Cell retention, viability and growth assays, chemotaxis assays, CD107a degranulation assays and ADCC assays were undertaken on ^{89}Zr-labeled and unlabeled NK cells (see Supplemental Data).

2. *In vivo* murine and PET/CT biodistribution studies

Animal experiments were ethically reviewed by an Animal Welfare & Ethical Review Board at King's College London and carried out in accordance with the Animals (Scientific Procedures) Act 1986 UK Home Office regulations governing animal experimentation. Eight- to ten-week-old female NOD-scid-gamma (NOD.Cg-Prkdc^{scid} Il2rg^{tm1Wjl}/SzJ) NSG mice (Charles River, UK) were inoculated with 1.5×10^6 HCC1954 cells in the left mammary fat pad between the 4th and 5th pairs of nipples. Experiments commenced when tumors reached 100-150 mm^3.

Tumor-bearing mice were randomized into three groups and intravenously administered 1×10^7 freshly radiolabeled NK cells (150-200 kBq), rhIL-15 (2500 IU), and either i) PBS, ii) anti-NIP isotype control (5 mg/kg), or iii) trastuzumab (5 mg/kg) (~200 µL PBS). NK cells from three healthy human volunteers were employed. Additional doses of rhIL-15 (2500 IU/dose) were given on days 3 and 6 via intra-peritoneal injection to support the *in vivo* survival and expansion of NK cells (*13*).

PET/CT imaging was conducted using a nanoScan PET-CT scanner (Mediso) on days 1, 3 and 7 post-cell injection. The images were co-registered and analyzed using VivoQuant v.3.0 (Invicro). SPECT/CT imaging using [^{111}In]In-CHX-A"-DTPA-trastuzumab was undertaken to determine the antibody biodistribution (Supplemental Data).

3. *Ex vivo* flow cytometric study

Single cell suspensions, prepared from mouse liver and spleen collected 3 days after ^{89}Zr-labeled NK cell administration, were stained with antihuman antibodies CD3-PE, CD56-FITC, CD16-APC, and CD45-PE-Cy7. CD45+ and CD45- populations were sorted (BD FACSMelody) and collected for γ-counting (Supplemental Data).

4. Statistical analysis

Independent experiments were conducted on separate days using NK cells from different donors. Statistical analysis was conducted using Prism 9.5.0 (GraphPad Software). Data were presented as mean ± standard deviation (SD). Statistical significance was determined using either unpaired or paired two-tailed Student's *t*-test. For tumor uptake analysis across the treatment groups, one-way analysis of

variance (ANOVA) followed by *t*-tests with multiple comparison correction (Tukey's method) was performed. A *P* value below 0.05 was considered statistically significant.

RESULTS

1. *In vitro* labeled ^{89}Zr-NK cells show comparable phenotype and functional characteristics to unlabeled NK cells

Using a prefabricated oxine kit (*15*), [^{89}Zr]Zr-oxine was reproducibly synthesized, with a radiochemical yield of 90.0 ± 5.8%. *Ex vivo* expanded human primary NK cells from peripheral blood were incubated with [^{89}Zr]Zr-oxine at room temperature for 15 min, with cell radiolabeling efficiencies of 42.2 ± 8.0%. The final specific activity measured 16.7 ± 4.7 kBq/10^6 cells.

To assess the effect of ^{89}Zr-labeling on human NK cells, several NK cell markers and functions were measured in ^{89}Zr-labeled NK (^{89}Zr-NK) cells, including phenotypic CD56 and CD16 expression and functional characteristics, namely migratory ability, viability and proliferation, and cytotoxic degranulation and ADCC responses. Flow cytometry of both ^{89}Zr-NK (measured at 2 h and 24 h post-radiolabeling) and unlabeled NK cells indicated that CD56 and CD16 expression was unaffected by ^{89}Zr-labeling (Figure 1A). The migration of ^{89}Zr-NK (24 h post-radiolabeling) and unlabeled NK cells towards FBS stimulus was similar, with migration towards FBS for both cells shown to be 3-4 fold higher than background migration (Figure 1B). The cytotoxic response of NK cells was measured in a degranulation assay by quantifying the levels of lysosome-associated membrane protein-1 (CD107a) (Figure 1C). The percentages of CD107a+ cells in both ^{89}Zr-NK cells and unlabeled NK cells were comparable across all conditions: high percentages in the PMA/Ionomycin positive controls (74.9 ± 8.7% and 77.8 ± 8.0%), moderate percentages in the presence of either HCC1954 (23.4 ± 11.0% and 21.5 ± 12.7%) or MDA-MB-231 (46.7.4 ± 7.4% and 47.6 ± 13.0%) co-cultures, and minimal baseline degranulation (2.4 ± 1.9% and 2.9 ± 2.4%).

The viability of ^{89}Zr-NK cells in culture, determined by trypan blue assay, remained unaffected (>95%) over 7 days, as compared to unlabeled NK cells (Figure 1D). However, in the absence of interleukins, ^{89}Zr-NK cells did not proliferate after radiolabeling, even at low levels of associated ^{89}Zr (~16 kBq/10^6 cells) (Figure 1E), whilst unlabeled NK cells continued to proliferate; the difference became significant from day 2 in culture ($P < 0.05$). Lastly, ^{89}Zr-radioactivity slowly dissociated from NK cells, with 73.7 ±

10.4% of the initial activity remaining in the cells at day 1, 58.9 ± 10.5% at day 3 and 36.4 ± 10.5% at day 7 (Figure 1F).

The cytolytic activity of ^{89}Zr-NK cells (24 h post-radiolabeling) and unlabeled NK cells, from four healthy human donors, was assessed in ADCC assays using trastuzumab and HER2-positive breast cancer cell lines SKBR3 and HCC1954 (Figure 2). For each donor, ^{89}Zr-NK cells displayed highly similar ADCC effects compared to unlabeled NK cells. Consistent with published literature, ADCC effects were donor-specific: trastuzumab boosted the cytolytic activity of NK cells from Donors A and B against both cell lines in a concentration-dependent manner, whereas negligible ADCC effects were observed for Donors C and D under our experimental conditions (Figure S1).

2. ^{89}Zr-NK cells in HCC1954 tumor-bearing mice demonstrate enhanced tumor localization with trastuzumab treatment

Using PET/CT imaging, the migration and accumulation of human ^{89}Zr-NK cells were studied in female NSG immunodeficient mice (which lack T, B and NK cells) bearing orthotopic human HCC1954 breast tumors. Despite expressing high levels of HER2, HCC1954 cells are resistant to the Fab-mediated HER2-binding downstream inhibitory (and associated therapeutic) effects of trastuzumab (*21*). Therefore, the HCC1954 model is useful in assessing trastuzumab treatment on NK cell tumor accumulation in a setting where the antibody can only exert Fc-mediated effector functions against these tumors.

Here, 1×10^7 ^{89}Zr-NK cells were co-administered to mice intravenously (tail vein) in combination with either a PBS sham (n = 6), HER2-targeted trastuzumab (n = 6) or a hapten-specific anti-NIP IgG1 isotype control antibody (n = 4) (which does not recognize mammalian antigens including HER2, but bears a human Fc region capable of binding to CD16 receptors of NK cells). NK cells from three different healthy volunteers were employed, with two animals in each group receiving ^{89}Zr-NK cells from each volunteer. Additionally, mice received intraperitoneal doses of rhIL-15 to support the survival of NK cells *in vivo* (*13*). PET/CT scanning was undertaken 1, 3 and 7 days post-injection (PI) of ^{89}Zr-NK cells.

In all mice, ^{89}Zr-NK cells migrated to the lungs, liver and spleen within the first 24 h, with redistribution from the lungs to the liver and spleen over 7 days (Figure 3A).

PET/CT imaging indicated that ^{89}Zr-NK cells accumulated in tumors but decreased from 1 day to 7 days PI. ^{89}Zr-NK cell tumor distribution was highly heterogeneous in all groups of mice. A significant proportion of ^{89}Zr-NK cells localized at the periphery of tumors (see **Supplemental Video Data**). Importantly, from PET quantification (Figure 3B), mice in the trastuzumab-treated group demonstrated significantly higher ^{89}Zr-NK cell infiltration in tumors at 1 day PI (0.66 ± 0.13 %ID.g^{-1}) compared to both the sham group (0.38 ± 0.16 %ID.g^{-1}, P = 0.0063) and the isotype group at 1 day PI (0.37 ± 0.11 %ID.g^{-1}, P = 0.0499). Similarly, at 3 days PI, the trastuzumab-treated group demonstrated higher ^{89}Zr-NK cell tumor infiltration (0.34 ± 0.12 %ID.g^{-1}) compared to the sham group (0.21±0.04 %ID.g^{-1}, P = 0.0593) and the isotype group (0.18 ± 0.03 %ID.g^{-1}, P = 0.0268). At the same time points, there was no significant difference in tumor activity between the isotype-treated group and the PBS sham-treated group. In concordance with the gradual loss of ^{89}Zr label observed following culture of ^{89}Zr-NK cells for 7 days *in vitro*, in this *in vivo* study, only low amounts of ^{89}Zr were detected in tumors 7 days PI (0.15 ± 0.04 %ID.g^{-1} in the trastuzumab group) and no differences between groups were found at this time point (Figure 3B).

Ex vivo biodistribution and tissue γ-counting experiments at days 3 and 7 provided similar results to PET image quantification, demonstrating comparable radioactivity concentrations in major organs and tissues (Figure S2). However, no significant differences in tumor radioactivity between trastuzumab-treated, PBS sham and isotype groups were found at day 3, likely due to loss of NK cells during washing steps following dissection, given their predominant localization in the tumor periphery.

3. ^{89}Zr-NK cells accumulate and persist in spleen and liver tissue

To validate this ^{89}Zr-NK PET imaging method, *ex vivo* flow cytometric phenotyping was undertaken. Liver and spleen tissues from mice administered ^{89}Zr-NK cells (3 days PI) were processed to form single cell suspensions, followed by staining. Flow cytometry (Figure 4) revealed the presence of human CD45+ cells, which were further identified as CD56+CD16+ NK cells. CD45+ and CD45- cell populations were separated and counted for radioactivity: human CD45+ cells from the liver measured an average of 1899 CPM/10^3 cells, whilst CD45- cells measured 0.9 CPM/10^3 cells; CD45+ cells from the spleen measured 1230 CPM/10^3 cells, whilst CD45- cells measured 0.8 CPM/10^3 cells. This indicated that ^{89}Zr signal was largely associated with human NK cells in soft tissue.

The accumulation of ^{89}Zr-NK cells was particularly high in the spleen across all groups, with ^{89}Zr radioactivity concentration highest in animals co-administered trastuzumab, at 3 and 7 days PI (Figure 3B). To interrogate this further, ^{89}Zr-NK cells were co-administered with an ^{111}In-labelled CHX-A"-DTPA-trastuzumab immunoconjugate. At 3 days PI, PET/CT and SPECT/CT showed co-localization of ^{89}Zr signal and ^{111}In signal (0.45 ± 0.001 %ID) in splenic tissue (Figure 5A). SPECT/CT imaging also indicated that significant amounts of [^{111}In]In-CHX-A"-DTPA-trastuzumab accumulated in HER2-positive HCC1954 tumors (2.41 ± 0.006 %ID). Importantly, heterogenous PET signal, attributed to infiltration of ^{89}Zr-NK cells, was coincident with SPECT signal of [^{111}In]In-CHX-A"-DTPA-trastuzumab in tumor tissue (Figure 5B).

Lastly, to confirm the presence of human NK cells in spleen, liver and tumors in this specific NSG orthotopic HCC1954 breast cancer murine model, NK cells were labeled *ex vivo* with fluorescent CMFDA, prior to intravenous *in vivo* administration, both with and without trastuzumab. Confocal microscopy of tumor, lung, spleen and liver sections, obtained 3 days PI and co-stained with DAPI, revealed the presence of CMFDA-labeled NK cells in these tissues (Figure 6, S3).

DISCUSSION

^{89}Zr-oxine (*19*) has been increasingly employed for PET tracking of immune cells, including NK, CAR-T, γδ-T and bone marrow cells (*16*,*17*). Here, the ^{89}Zr radiolabeling yields and *in vitro* cellular retention of NK cells were comparable to that of previous studies of NK cells (*14*) and other immune cells (*17*). Importantly, the average specific activity of ^{89}Zr-NK cells employed here did not significantly alter crucial functional NK cell characteristics, including NK cellular viability, motility, activation and cytolytic potency, alongside key phenotypic markers, consistent with prior reports (*14*). Although *in vitro* retention of ^{89}Zr radioactivity decreased over 7 days, retention at days 1 and 3 was sufficiently high to enable reliable *in vivo* ^{89}Zr-NK cell PET tracking.

PET/CT images revealed initial margination of ^{89}Zr-NK cells in lung – the first capillary bed encountered by intravenously injected cells – followed by redistribution to liver and spleen. This is consistent with many prior cell tracking reports (*11*–*14*) (Table S1).

Additionally, ^{89}Zr activity accumulated in the mouse bones, most prominently in the joints, consistent with reports that dissociated, oxyphilic Zr^{4+} is associated with regions of high bone mineralization (*22*). It is highly probable that a portion of this signal is indeed a result of NK cell migration to the bone marrow (*11*). In addition, our *ex vivo* flow cytometric evaluations demonstrated that NK cells isolated from liver and spleen tissues showed 1500-fold and 2100-fold higher levels of ^{89}Zr radioactivity compared to murine spleen and liver cells respectively, indicating that in soft tissue, ^{89}Zr activity is largely associated with only the administered human NK cells.

Prior imaging studies in murine cancer models and cancer patients, showing the migration of pre-labeled NK cells to tumors, are consistent with our data. NIR optical imaging has indicated the *in vivo* migration of NIR dye-labeled human NK cells to human MDA-MB-231 breast tumors in NSG mice (*8*). Whole-body SPECT imaging studies in patients with renal cell carcinoma have evidenced that ^{111}In-labeled allogenic NK cells migrate to metastases (*11*).

We show that ^{89}Zr-NK cells migrate to HCC1954 breast cancer xenografts, *with or without trastuzumab treatment*. At 1 and 3 days PI, enhanced NK cell infiltration in tumor tissue is associated with co-administration of trastuzumab, aligning with clinical evidence (*1*,*2*,*7*). However, although statistically significant, this enhancement remains relatively modest. Several mechanisms could restrict NK cell tumor infiltration. In solid tumors, such as ovarian carcinoma and lung cancer, NK cell activation by anti-tumor antibody therapy is limited (*23*–*25*). NK cells may be exhausted in the tumor microenvironment due to the downregulation of activation markers (*26*), leading to reduced infiltration and retention. Alternatively, upon activation, CD16 can be shed or sequestered, thus modulating ADCC effects (*27*).

Animals co-administered trastuzumab demonstrated higher splenic uptake of ^{89}Zr-NK cells compared to animals co-administered a PBS-sham, at 3 and 7 days PI. SPECT/CT indicated that significant amounts of [^{111}In]In-CHX-A"-DTPA-trastuzumab also localized to the spleen. Splenic vasculature is highly perfused and permeable to many blood-borne components: immune cells (*11*–*14*) and IgG antibodies (*28*) are well-documented to accumulate in splenic tissue. In immune-deficient NSG mice that lack B-cells and therefore normal endogenous levels of circulating immunoglobulins, exogenous human IgG antibodies exhibit particularly high uptake in the spleen. This has been attributed to antibody Fc binding to unoccupied murine FcRs expressed on spleen-residing monocytes, neutrophils, macrophages and dendritic cells (*29*). In this study, it is possible that high residency of trastuzumab

antibody in the spleen increases the accumulation of human ^{89}Zr-NK cells, which can compete with endogenous immune cells for binding to the humanized trastuzumab Fc region. However, we note that animals co-administered an IgG isotype control alongside ^{89}Zr-NK cells, did not show the same levels of splenic ^{89}Zr activity as that of animals co-administered trastuzumab.

Multiple doses of NK cells combined with antibody treatment can augment ADCC effects better than a single dose of NK cells or multiple doses of antibody alone (*27*). Future studies of different dosing regimens of ^{89}Zr-NK cells and antibody will allow more in-depth studies of cellular dynamics in the context of therapy.

CONCLUSIONS

We have shown the utility of [^{89}Zr]Zr-oxine for radiolabeling and tracking of human NK cells in a murine orthotopic human breast cancer model. This sensitive method enables quantitative assessment of changes in NK cell biodistribution in response to antibody therapies. Importantly, our findings reveal that NK cells migrate to orthotopic HER2-expressing HCC1954 tumors, with enhanced infiltration facilitated by HER2-targeted trastuzumab at early time points, aligning with clinical evidence. The use of ^{89}Zr and PET/CT can therefore aid the development and understanding of antibody therapies, in the context of the immune environment and Fc-mediated therapeutic effects.

DISCLOSURE: This research was supported by Cancer Research UK (C30122/A11527; C30122/A15774; C4278/A27066) including a Career Establishment Award (C63178/A24959), the EPSRC (EP/S032789/1), Wellcome Trust (WT212885/Z/18/Z; WT201959/Z/16/Z; WT088641/Z/09/Z), Breast Cancer Now (147KL-Q3) and the MRC (MR/L023091/1, MR/N013700/1). PJB has submitted a patent application related to [^{89}Zr]^{89}Zr-Oxine technology. SNK is a founder and shareholder of Epsilogen Ltd. and declares patents on antibody technologies. No other potential conflicts of interest relevant to this article exist.

ACKNOWLEDGEMENTS

We thank Anthony Cheung for feedback on this manuscript.

KEY POINTS:

QUESTION: Can PET/CT assess [^{89}Zr]Zr-oxine labeled human NK cell infiltration in HER2-positive breast tumors and quantify whether HER2-targeted trastuzumab therapy enhances this infiltration?

PERTINENT FINDINGS: ^{89}Zr-NK cells migrate to orthotopic HER2-expressing HCC1954 human tumors, with enhanced infiltration facilitated by HER2-targeted trastuzumab at early time points, aligning with clinical evidence.

IMPLICATIONS FOR PATIENT CARE: The use of ^{89}Zr and PET/CT can aid the development and understanding of antibody therapies, in the context of the immune environment and Fc-mediated therapeutic effects.

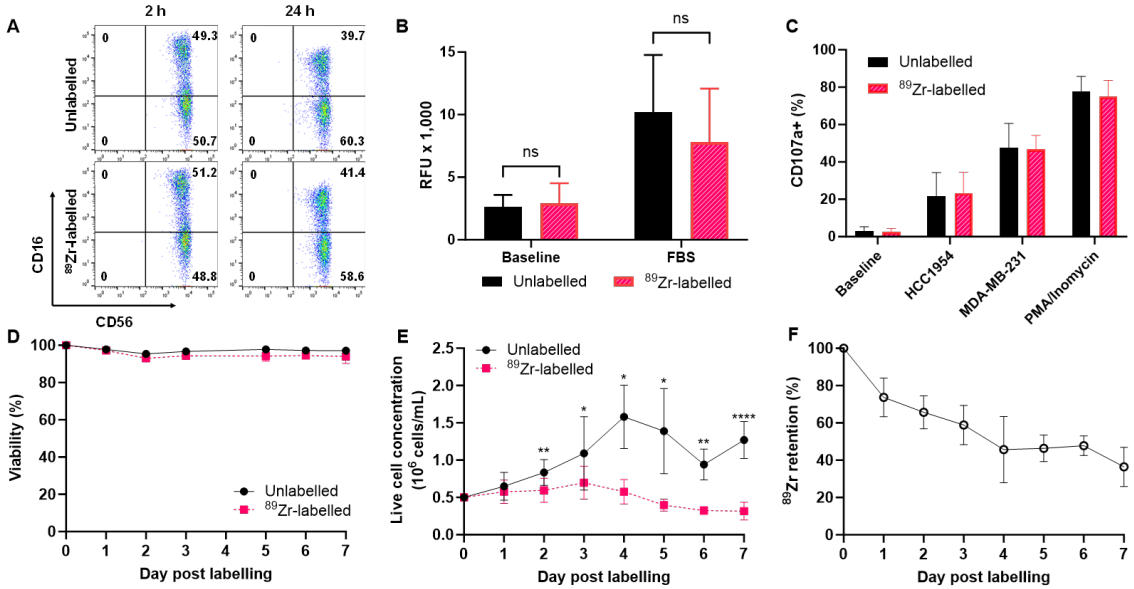

Figure 1. *In vitro* functional and phenotypic characteristics of ^{89}Zr-NK cells and ^{89}Zr-retention. **(A)** Flow cytometry shows comparable CD56 and CD16 expression in unlabeled and ^{89}Zr-NK cells. **(B)** Chemotaxis assays show that chemotactic responses to FBS, in unlabeled and ^{89}Zr-NK cells, are similar (mean ± SD, *n* = 5). **(C)** Degranulation assays reveal similar degranulation levels in ^{89}Zr-NK and unlabeled NK cells under various conditions (mean ± SD, *n* = 4). **(D)** Viability and **(E)** proliferation profiles indicate that both ^{89}Zr-NK and unlabeled NK cells remained viable for up to 7 days in culture without interleukins. Whilst unlabeled NK cells continued to proliferate, ^{89}Zr-NK cells did not. (mean ± SD, *n* = 7). **(F)** ^{89}Zr retention in ^{89}Zr-NK cells gradually decreased over 7 days in culture, with 36.4 ± 10.5% of the initial activity remaining on day 7 (mean ± SD, *n* = 7). ns = non-significant, **P* < 0.05, ***P* < 0.01, *****P* < 0.0001.

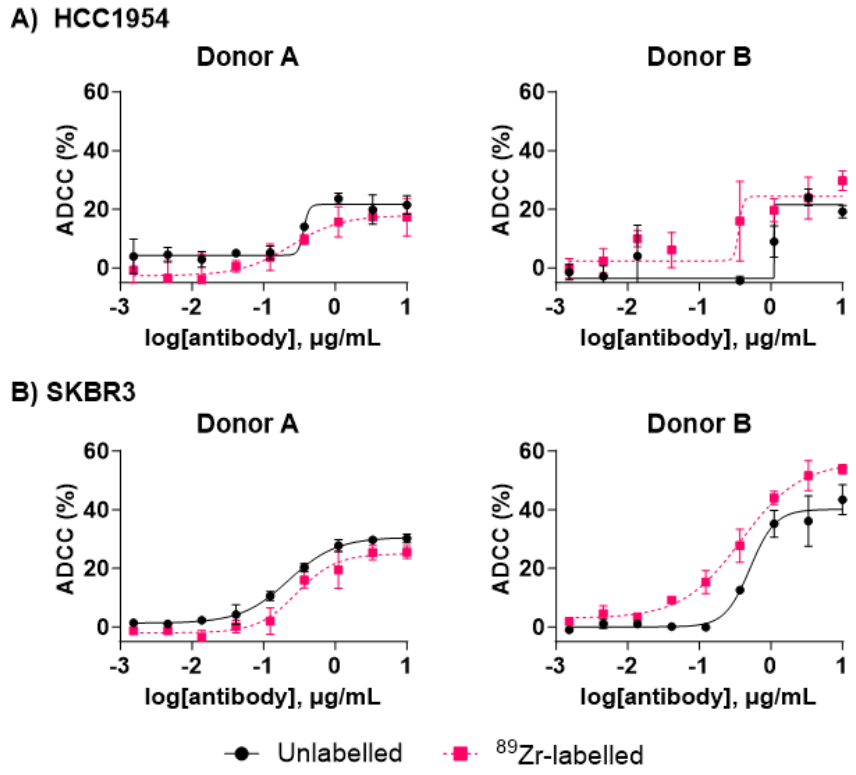

Figure 2. ADCC assays using ^{89}Zr-labeled and unlabeled NK cells against HER2-expressing breast cancer cell lines **(A)** HCC1954 and **(B)** SKBR3 (10:1 effector:target ratio) and various trastuzumab concentrations. ^{89}Zr-NK cells demonstrated a similar ADCC response to unlabeled NK cells. The ADCC response varied amongst human NK cells from different healthy volunteers. Also see Figure S1. ADCC = Antibody-Dependent Cell-mediated Cytotoxicity. Data was fitted to a four-parameter logistic curve.

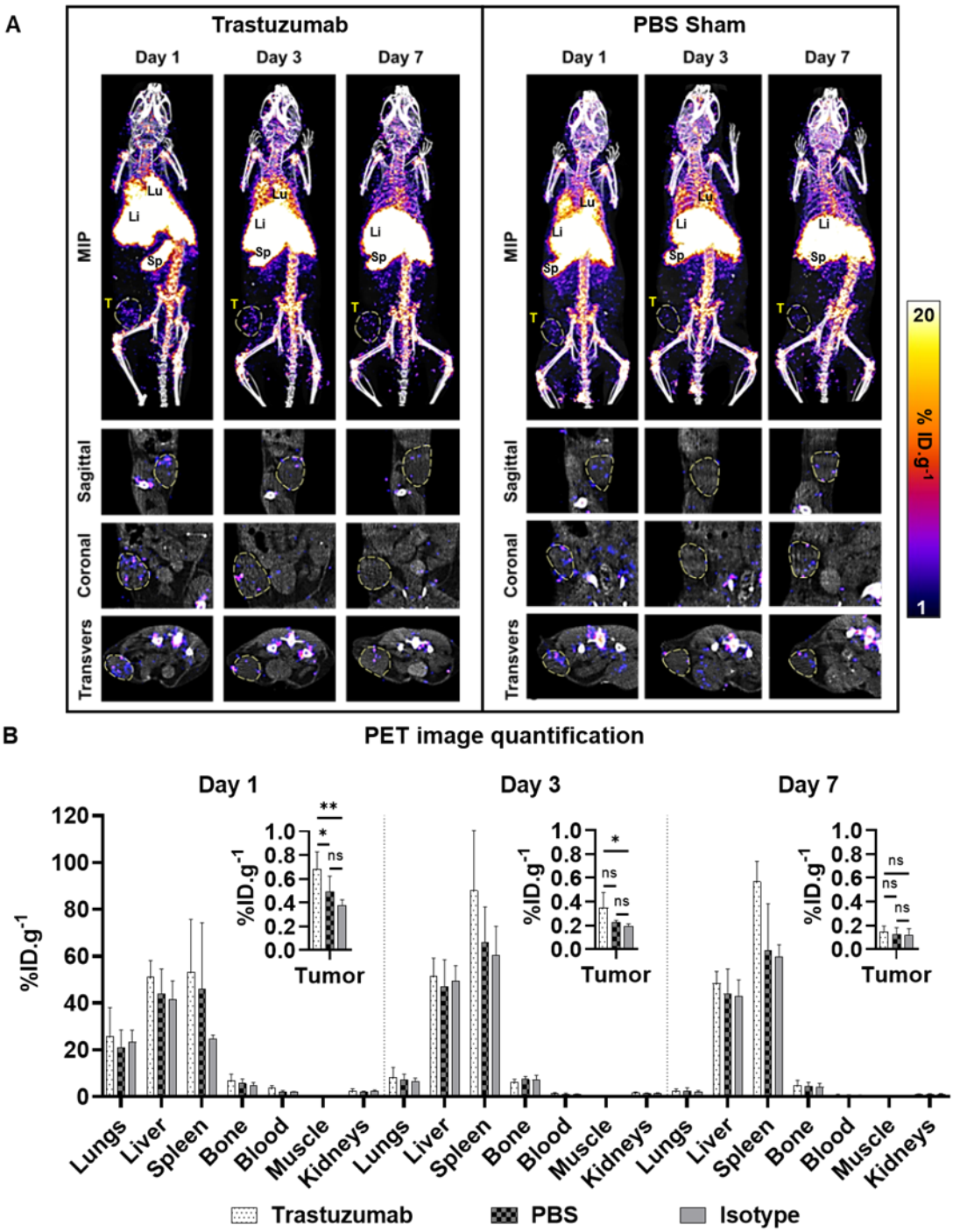

Figure 3. Biodistribution of ^{89}Zr-NK cells in female NSG mice bearing orthotopic HER2-expressing HCC1954 tumors. **(A)** Representative Maximum Intensity Projections and tumor slice PET/CT images of mice administered ^{89}Zr-NK cells (10^7 cells, ~150-200 kBq) in combination with trastuzumab (5 mg/kg), or phosphate buffered saline (PBS) only. Li = Liver, Lu = Lungs, Sp = Spleen, T = Tumor. Tumors are outlined for clarity. **(B)** PET image quantification of selected organs and tumors (mean ± SD, *n* = 4-6/group. **P* < 0.05, ***P* < 0.01).

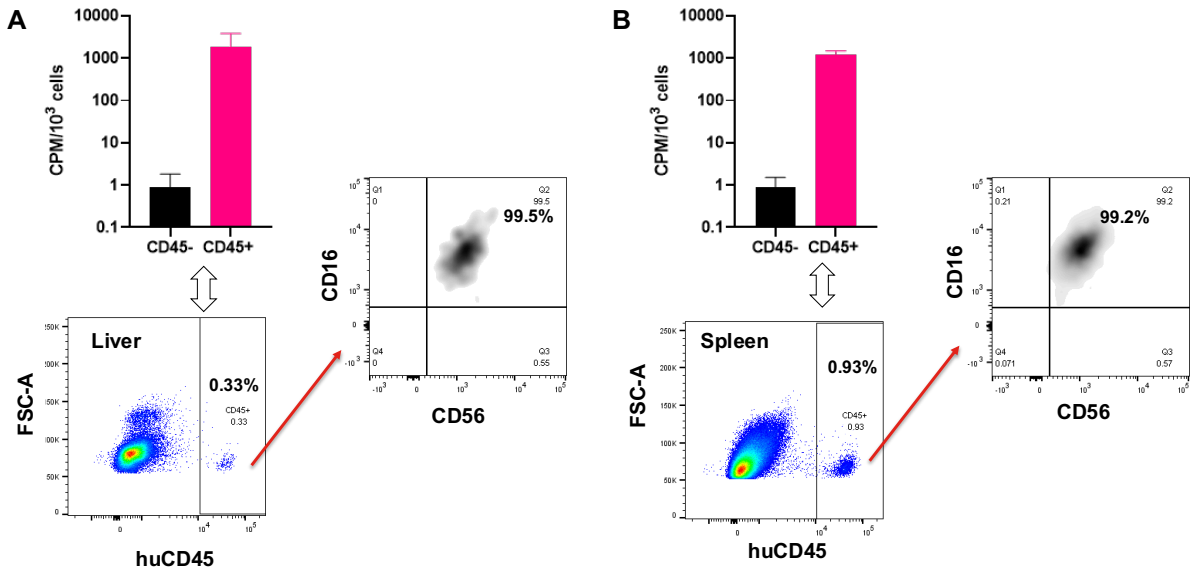

Figure 4. Flow cytometry and γ-counting of CD45+ and CD45- cell populations from murine **(A)** liver and **(B)** spleen revealed that ^{89}Zr radioactivity was associated with human CD45+ cells (*n* = 4, mean ± SD), which were confirmed as C56+CD16+ NK cells. CPM = counts per minute.

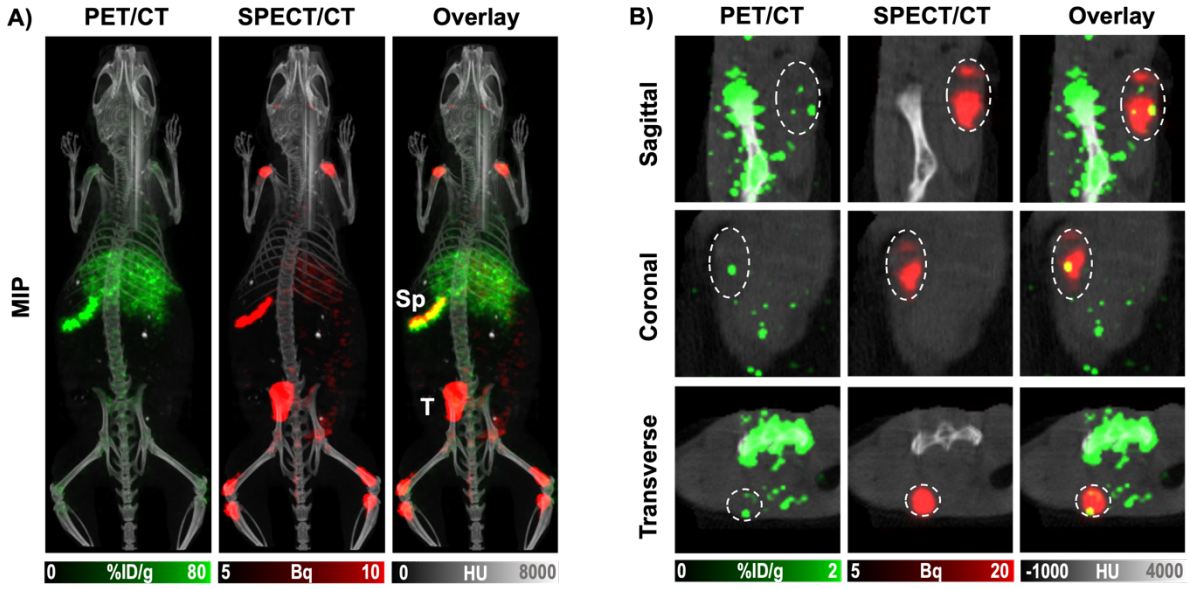

Figure 5. **(A)** Maximum Intensity Projections and **(B)** tumor slice PET/CT and SPECT/CT images of mice 3 days PI of ^{89}Zr-NK cells in combination with [^{111}In]In-CHX-A"-DTPA-trastuzumab. Sp = Spleen, T = Tumor.

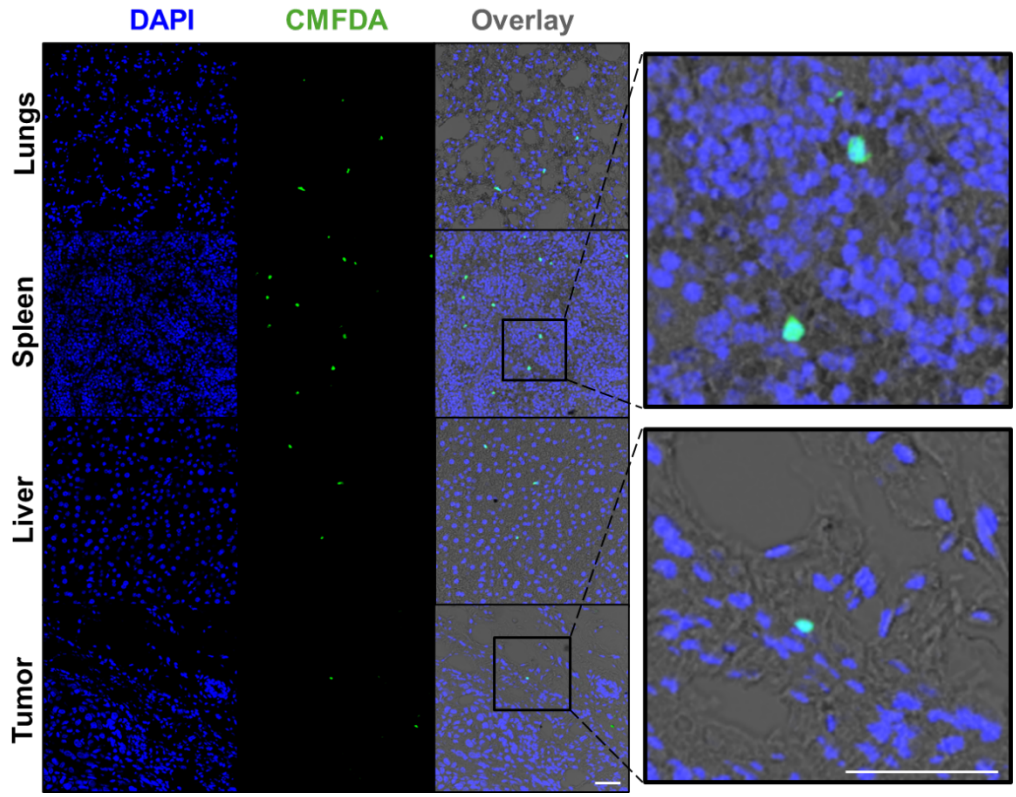

Figure 6. Confocal microscopy images (40× magnification) of tumor, lung, spleen and liver sections, 3 days PI of NK cells and trastuzumab. Sections, stained with DAPI, revealed the presence of CMFDA-labeled NK cells. Scale bar = 50 μm.

REFERENCES

1. Gennari R, Menard S, Fagnoni F, et al. Pilot study of the mechanism of action of preoperative trastuzumab in patients with primary operable breast tumors overexpressing HER2. *Clin Cancer Res*. 2004;10:5650-5655.

2. Arnould L, Gelly M, Penault-Llorca F, et al. Trastuzumab-based treatment of HER2-positive breast cancer: an antibody-dependent cellular cytotoxicity mechanism? *Br J Cancer 2006 942*. 2006;94:259-267.

3. Muntasell A, Rojo F, Servitja S, et al. NK cell infiltrates and HLA class I expression in primary HER2 breast cancer predict and uncouple pathological response and disease-free survival. *Clin Cancer Res*. 2019;25:1535-1545.

4. Loi S, Michiels S, Salgado R, et al. Tumor infiltrating lymphocytes are prognostic in triple negative breast cancer and predictive for trastuzumab benefit in early breast cancer: Results from the FinHER trial. *Ann Oncol*. 2014;25:1544-1550.

5. Denkert C, von Minckwitz G, Darb-Esfahani S, et al. Tumour-infiltrating lymphocytes and prognosis in different subtypes of breast cancer: a pooled analysis of 3771 patients treated with neoadjuvant therapy. *Lancet Oncol*. 2018;19:40-50.

6. Uong TNT, Lee K-H, Ahn S-J, et al. Real-time tracking of ex vivo-expanded natural killer cells toward human triple-negative breast cancers. *Front Immunol*. 2018;9:825.

7. Uong TNT, Yoon MS, Lee K-H, et al. Live cell imaging of highly activated natural killer cells against human hepatocellular carcinoma in vivo. *Cytotherapy*. 2021;23:799-809.

8. Hosahalli Vasanna S, Perera R, Jackson Z, Abenojar E, Exner A, Wald D. Non-invasive tracking of nanobubble tagged natural killer cells using clinical ultrasound. *Blood*. 2022;140:10283-10284.

9. Meller B, Frohn C, Brand JM, et al. Monitoring of a new approach of immunotherapy with allogenic ^{111}In-labelled NK cells in patients with renal cell carcinoma. *Eur J Nucl Med Mol Imaging*. 2004;31:403-407.

10. Matera L, Galetto A, Bello M, et al. In vivo migration of labeled autologous natural killer cells to

liver metastases in patients with colon carcinoma. *J Transl Med*. 2006;4:49.

11. Cany J, van der Waart AB, Tordoir M, et al. Natural killer cells generated from cord blood hematopoietic progenitor cells efficiently target bone marrow-residing human leukemia cells in NOD/SCID/IL2Rgnull mice. *PLoS One*. 2013;8:e64384.

12. Sato N, Stringaris K, Davidson-Moncada JK, et al. In vivo tracking of adoptively transferred natural killer cells in rhesus macaques using ^{89}zirconium-oxine cell labeling and PET imaging. *Clin Cancer Res*. 2020;26:2573-2581.

13. Man F, Khan AA, Carrascal-Miniño A, Blower PJ, T.M. de Rosales R. A kit formulation for the preparation of [^{89}Zr]Zr(oxinate)$_4$ for PET cell tracking: White blood cell labelling and comparison with [^{111}In]In(oxinate)$_3$. *Nucl Med Biol*. 2020;90-91:31-40.

14. Weist MR, Starr R, Aguilar B, et al. PET of adoptively transferred chimeric antigen receptor T Cells with ^{89}Zr-Oxine. *J Nucl Med*. 2018;59:1531-1537.

15. Man F, Lim L, Volpe A, et al. In vivo PET tracking of ^{89}Zr-labeled Vγ9Vδ2 T Cells to mouse xenograft breast tumors activated with liposomal alendronate. *Mol Ther*. 2019;27:219-229.

16. Asiedu KO, Koyasu S, Szajek LP, Choyke PL, Sato N. Bone marrow cell trafficking analyzed by ^{89}Zr-oxine Positron Emission Tomography in a murine transplantation model. *Clin Cancer Res*. 2017;23:2759-2768.

17. Sato N, Wu H, Asiedu KO, Szajek LP, Griffiths GL, Choyke PL. ^{89}Zr-Oxine complex PET cell imaging in monitoring cell-based therapies. *Radiology*. 2015;275:490-500.

18. Charoenphun P, Meszaros LK, Chuamsaamarkkee K, et al. [^{89}Zr]Oxinate$_4$ for long-term in vivo cell tracking by positron emission tomography. *Eur J Nucl Med Mol Imaging*. 2015;42:278-287.

19. Miltenyi Biotec. NK cells expansion from human PBMCs or isolated NK cells. https://www.miltenyibiotec.com/GB-en/applications/all-protocols/nk-cell-expansion-from-human-pbmcs-or-isolated-nk-cells.html. Accessed Oct 2, 2020.

20. O'Brien NA, Browne BC, Chow L, et al. Activated phosphoinositide 3-kinase/AKT signaling confers resistance to trastuzumab but not lapatinib. *Mol Cancer Ther*. 2010;9:1489-1502.

21. Ma MT, Meszaros LK, Paterson BM, et al. Tripodal tris(hydroxypyridinone) ligands for

immunoconjugate PET imaging with $^{89}Zr^{4+}$: comparison with desferrioxamine-B. *Dalton Trans*. 2015;44:4884-4900.

22. Lee SC, Shimasaki N, Lim JSJ, et al. Phase I trial of expanded, activated autologous NK-cell infusions with trastuzumab in patients with HER2-positive cancers. *Clin Cancer Res*. 2020;26:4494-4502.

23. Szmania S, Lapteva N, Garg T, et al. Ex vivo–expanded Natural Killer cells demonstrate robust proliferation in vivo in high-risk relapsed multiple myeloma patients. *J Immunother*. 2015;38:24-36.

24. Hu W, Wang G, Huang D, Sui M, Xu Y. Cancer immunotherapy based on natural killer cells: Current progress and new opportunities. *Front Immunol*. 2019;10:1205.

25. Tong L, Jiménez-Cortegana C, Tay AHM, Wickström S, Galluzzi L, Lundqvist A. NK cells and solid tumors: therapeutic potential and persisting obstacles. *Mol Cancer*. 2022;21:1-18.

26. Ran G he, Lin Y qing, Tian L, et al. Natural killer cell homing and trafficking in tissues and tumors: from biology to application. *Signal Transduct Target Ther 2022 71*. 2022;7:1-21.

27. Zhu H, Blum RH, Bjordahl R, et al. Pluripotent stem cell-derived NK cells with high-affinity noncleavable CD16a mediate improved antitumor activity. *Blood*. 2020;135:399-410.

28. Cataldi M, Vigliotti C, Mosca T, Cammarota MR, Capone D. Emerging role of the spleen in the pharmacokinetics of monoclonal antibodies, nanoparticles and exosomes. *Int J Mol Sci*. 2017;18:1249.

29. Sharma SK, Chow A, Monette S, et al. Fc-mediated anomalous biodistribution of therapeutic antibodies in immunodeficient mouse models. *Cancer Res*. 2018;78:1820-1832.

GRAPHICAL ABSTRACT